JOURNAL OF SOLID STATE CHEMISTRY 60, 332–342 (1985)

Structure and Properties of $Y_5Mo_2O_{12}$ and $Gd_5Mo_2O_{12}$: Mixed Valence Oxides with Structurally Equivalent Molybdenum Atoms

C. C. TORARDI*

Central Research and Development Department, †E. I. du Pont de Nemours and Company, Experimental Station, Wilmington, Delaware 19898

C. FECKETTER AND W. H. McCARROLL*

Department of Chemistry, Rider College, P.O. Box 6400, Lawrenceville, New Jersey 08648

AND F. J. DiSALVO

AT&T Bell Laboratories, 600 Mountain Avenue, Murray Hill, New Jersey 07974

Received May 28, 1985

Crystals of $Ln_5Mo_2O_{12}$ (Ln = Y, Gd) were grown by electrochemical reduction of alkali-molybdate/rare-earth oxide melts at 1075–1100°C. A single crystal of $Y_5Mo_2O_{12}$, used for structure determination, was found to be monoclinic with a = 12.2376(7) Å, b = 5.7177(8) Å, c = 7.4835(5) Å, β = 108.034(5)°, and Z = 2. Although the structure was refined in space group $C2/m$, the true space group appears to be $P2_1/m$. In $Y_5Mo_2O_{12}$, rutile-like sheets of edge-shared MoO_6 chains linked by YO_6 octahedra are interconnected with YO_7 monocapped trigonal prisms. The Mo atoms in the chains have alternating distances of 2.496 and 3.221 Å and in that respect are similar to MoO_2. However, in contrast to metallic MoO_2 both the Y and Gd compounds are n-type semiconductors with room temperature resistivities of the order of 10^3 ohm–cm. Magnetic susceptibility measurements confirm the presence of one unpaired electron per Mo_2 unit. The semiconducting behavior can be explained in terms of an unfavorable bridging oxygen coordination which prevents electron delocalization through metal–oxygen pi bonding as in MoO_2.

Introduction

During the past several years, a number of reports have appeared which reveal a rich and varied chemistry for the reduced oxides of molybdenum in combination with the rare earths and yttrium (*1–12*). For the most part, these compounds have been prepared by methods which yield only polycrystalline products and, as a result, their structures are either unknown or have been inferred from X-ray powder diffraction data. One such series of compounds re-

* To whom correspondence may be addressed.
† Contribution 3789.

0022-4596/85 $3.00

ported several years ago as having the composition Ln_2MoO_5 (*Ln* = a trivalent rare earth or ytrrium) has a monoclinic unit cell very similar to that reported for a similar series of tetravalent rhenium oxides such as Ln_2ReO_5 (*13*). Although their structures were not known, members of both series were reported to have anomalously low magnetic moments which suggested the possible presence of strong transition metal interactions (*4, 5, 9, 13*).

Recently, one of us (*14*) reported that fused salt electrolysis can be used for the synthesis of reduced oxides of molybdenum with lanthanum, neodymium, and yttrium. Since they included the ytrrium phase discussed above, a determination of its structure was undertaken. Early on in the single crystal diffraction study it became clear that the unit cell contained 10 yttrium atoms and only 4 molybdenum atoms and that the true formula was $Y_5Mo_2O_{12}$. A subsequent check of the literature revealed a recent structural report by Baud *et al.* (*15, 16*) for a compound having the composition $Dy_5Re_2O_{12}$ whose unit cell parameters appear to be essentially identical to those reported for Dy_2MoO_5. Although they were able to accurately determine the positions of the heavy atoms, polysynthetic twinning prevented a satisfactory refinement and as a result the positions of the oxygen atoms were not accurately determined. Such twinning was not a problem in the study reported here for $Y_5Mo_2O_{12}$ and a successful refinement was achieved. The results of this study are presented below together with supporting electrical and magnetic data for both the yttrium and the isomorphous gadolinium compound.

Experimental

1. Synthesis

Single crystals of $Y_5Mo_2O_{12}$ and $Gd_5Mo_2O_{12}$ were prepared by the electrolytic reduction of melts prepared from mixtures of sodium or lithium molybdate, molybdenum (VI) oxide, and the appropriate rare-earth oxide. The melt was contained in a high density alumina crucible. Smooth platinum foil electrodes with nominal surface areas of 1 cm^2 were used. Details of the technique are given elsewhere (*14*). Starting molar ratios of reactants, temperatures, current–voltage conditions, and times for the various electrolyses are given below:

Sample A. $Li_2MoO_4 : MoO_3 : Y_2O_3$ = 1.30 : 3.00 : 1.45; 1090°C, 2.0 V, 400 ma, 40 min.

Sample B. $Na_2MoO_4 : MoO_3 : Y_2O_3$ = 3.00 : 3.00 : 1.50; 1075°C, 1.1 V, 100 ma, 1 hr.

Sample C. $Na_2MoO_4 : MoO_3 : Gd_2O_3$ = 3.00 : 3.00 : 1.50; 1075°C, 1.1 V, 100 ma, 1 hr.

The cathode product was leached with alternate portions of hot 5% K_2CO_3 solution and hot 2 *M* HCl to remove the matrix and various unknown reduced materials, and in the case of the gadolinium preparation, $Gd_5Mo_3O_{16}$. The crystal used for the X-ray structure determination was selected from sample A prior to the realization of any compositional problems. The other samples which were used for chemical analysis and density determinations were treated with warm 6 *M* HNO_3 to remove MoO_2 which was sometimes observed as a polycrystalline coating or as small occluded crystals. Typically, the crystals grow as needles or crystalline laminates up to 1–3 mm in the largest dimension with the Gd samples on the average being somewhat larger than the Y compound. Twinning along the needle axis was common but single crystal fragments could easily be separated.

Solid-state reactions were run using intimately mixed stoichiometric quantities of freshly fired reactants which were pelleted and sealed in evacuated silica capsules. Products were fired at temperatures ranging from 1000–1250°C for several days with at

least one regrinding in between in an effort to achieve homogeneity. The rare-earth oxides were obtained from Rhone Poulenc Chemical Company and were ignited at 1000°C before use. All other chemicals were of reagent grade except the Li_2MoO_4 (Alfa Products, stated purity 98.5%) which was doubly recrystallized before use and the ZrO_2 (MCB) was stated to contain up to 2% hafnium.

2. Chemical Analysis

The portions of samples B and C which were used for chemical analysis were of a size that did not pass through a 50-mesh screen. These were carefully culled until visually homogeneous under the microscope, ground lightly, and subjected to final additional washes with hot K_2CO_3 and HCl solutions followed by warm 6 *M* HNO_3. Their X-ray diffraction patterns showed only the lines of the title compounds. The samples were dissolved in hot concentrated sulfuric acid which was evaporated to fumes of SO_3. Quantitative analyses for principal metallic constituents were carried out using standard volumetric methods. The rare earths were determined by titration using EDTA while molybdenum was determined by the Jones reductor method using ceric sulfate as the titrating agent.

Analysis. Calc. for $Y_5Mo_2O_{12}$: Y, 53.66; Mo, 23.16. Found: Y, 53.38; Mo, 23.07. Calc. for $Gd_5Mo_2O_{12}$: Gd, 67.19; Mo, 16.40; Found: Gd, 67.14; Mo, 16.49.

3. Electrical and Magnetic Measurements

The magnetic susceptibility of $Y_5Mo_2O_{12}$ was measured from 4.2 to 300 K using the Faraday method. Details of the experiment have been described earlier (*17*). Electrical resistivities of single crystals were measured using a four-point probe method. Current was passed parallel to the long axis of the tabletlike crystal which corresponded to the crystallographic unique axis.

4. X-Ray Powder Diffraction

X-Ray powder diffraction patterns for routine identification purposes were obtained using a Philips diffractometer and filtered copper radiation. Precision lattice constants were obtained with a Guinier–Hägg type focusing camera (r = 40 mm). The radiation was monochromatic Cu$K_{\alpha 1}$ (λ = 1.5405 Å) and the internal standard was Si (a = 5.4305 Å). An Optronics P-1700 Photomation instrument was used to collect absorbance data from the films. Peak positions and relative intensities were determined with local computer programs. The lattice parameters were refined by a least-squares procedure. Indexed X-ray powder diffraction patterns of $Y_5Mo_2O_{12}$ and $Gd_5Mo_2O_{12}$ recorded at room temperature are given in Tables I and II, respectively. All observed lines of $Y_5Mo_2O_{12}$ can be indexed on the basis of *C*-centered monoclinic symmetry with a = 12.243(2), b = 5.7197(6), c = 7.489(1) Å, and β = 107.99(1)°, Z = 2, V = 498.8(2) Å^3, $d_{X\text{-ray}}$ = 5.52 g · cm^{-3}, and d_{pyc} = 5.55(2) g · cm^3. Two very weak reflections in the $Gd_5Mo_2O_{12}$ powder diffraction pattern did not obey the *C*-centering requirement but it could be indexed in space group $P2_1/m$ with a = 12.431(2), b = 5.7748(5), c = 7.610(2) Å, β = 107.95(1)°, Z = 2, V = 519.7(2) Å^3, $d_{X\text{-ray}}$ = 7.48 g · cm^{-3}, and d_{pyc} = 7.58(2) g · cm^{-3}.

5. Single Crystal X-Ray Structure Determination[1]

A columnar-shaped single crystal of $Y_5Mo_2O_{12}$ with dimensions 0.067 × 0.093 × 0.267 mm was mounted with its long dimension parallel with the ϕ axis on an Enraf–Nonius CAD4 X-ray diffractometer equipped with monochromatic MoK_α radia-

[1] All crystallographic calculations were performed on a Digital Equipment Corporation VAX 11/780 computer using a system of programs developed by J. C. Calabrese. Structural plots were made with the ORTEP program (C. K. Johnson, 1976).

TABLE I

X-RAY POWDER DIFFRACTION DATA FOR $Y_5Mo_2O_{12}$

2θ	I(obs)	h k l	d(obs)	d(calc)
12.341	16	0 0 1	7.166	7.123
15.132	4	2 0 0	5.850	5.822
16.351	22	−2 0 1	5.417	5.398
19.831	3	−1 1 1	4.473	4.463
22.454	23	2 0 1	3.956	3.950
22.561	8	1 1 1	3.938	3.919
24.898	32	−2 0 2	3.573	3.568
		0 0 2		3.561
27.296	5	−3 1 1	3.264	3.256
27.724	98	3 1 0	3.215	3.212
28.346	100	−1 1 2	3.146	3.133
29.271	9	−4 0 1	3.048	3.044
30.662	43	4 0 0	2.913	2.911
31.231	15	0 2 0	2.861	2.860
32.358	18	−3 1 2	2.764	2.762
32.419	12	1 1 2	2.759	2.756
33.142	61	−4 0 2	2.701	2.700
33.209	40	2 0 2	2.695	2.691
33.716	55	0 2 1	2.656	2.654
34.897	40	2 2 0	2.569	2.567
35.470	33	−2 2 1	2.529	2.527
36.118	5	−2 0 3	2.485	2.483
36.728	3	4 0 1	2.445	2.443
38.815	17	2 2 1	2.318	2.316
39.556	12	−1 1 3	2.276	2.276
40.390	92	−2 2 2	2.231	2.231
		0 2 2		2.230
41.826	18	5 1 0	2.158	2.157
42.285	11	−5 1 2	2.136	2.135
42.396	5	3 1 2	2.130	2.130
43.364	24	−4 2 1	2.085	2.084
44.079	1	1 1 3	2.053	2.051
plus 52 lines to d(obs) = 1.263				

tion. After careful crystal alignment, 25 reflections were located and used to obtain cell parameters and orientation matrix. The reflections were indexed in a monoclinic cell with dimensions $a = 12.2376(7)$ Å, $b = 5.7177(8)$ Å, $c = 7.4835(5)$ Å, and $\beta = 108.034(5)°$. For $Z = 2$, the calculated density of 5.53 g · cm^{-3} compares well with the observed pycnometrically determined density of 5.55(2) g · cm^{-3}.

A total of 3196 reflections were collected at ambient temperature by the ω mode from $2° < \theta < 30°$ and merged to yield 877 independent data with $I \geq 3\sigma(I)$ in $2/m$ symmetry. The data were treated in the usual fashion for Lorentz and polarization effects. A correction for absorption was also applied using a Gaussian grid of 8 × 8 × 8. The crystal faces and distances (mm) from the center were ±[100, 0.033; 010, 0.133; 001, 0.047]. The transmission factors for the crystal ($\mu = 314.3$ cm^{-1}) varied from 0.0537 to 0.1783.

An examination of the data revealed the presence of a dominant *C*-centered lattice. This was also observed in precession photographs of the same crystal which showed several weak spots with $h + k = 2n + 1$. Of

TABLE II

X-RAY POWDER DIFFRACTION DATA FOR $Gd_5Mo_2O_{12}$

2θ	I(obs)	h k l	d(obs)	d(calc)
14.963	9	2 0 0	5.916	5.913
16.145	16	−2 0 1	5.485	5.482
22.135	18	2 0 1	4.013	4.013
22.378	16	1 1 1	3.970	3.971
24.542	26	−2 0 2	3.624	3.625
26.967	7	−3 1 1	3.303	3.300
27.399	99	3 1 0	3.252	3.256
28.084	100	−1 1 2	3.175	3.177
28.700	39	−4 0 1	3.108	3.091
30.204	41	4 0 0	2.956	2.956
30.923	54	0 2 0	2.889	2.887
31.954	41	1 1 2	2.798	2.797
32.676	97	−4 0 2	2.738	2.741
33.389	59	0 2 1	2.681	2.682
34.182	11	4 1 0	2.621	2.631
34.538	51	2 2 0	2.595	2.594
35.107	24	−2 2 1	2.554	2.555
38.375	13	2 2 1	2.344	2.344
38.952	15	−1 1 3	2.310	2.311
39.908	72	0 2 2	2.257	2.257
41.213	34	5 1 0	2.189	2.189
41.673	15	−5 1 2	2.165	2.167
42.821	17	−4 2 1	2.110	2.110
43.787	10	4 2 0	2.066	2.066
45.048	9	−6 0 2	2.011	2.011
45.619	73	−4 2 2	1.987	1.988
46.016	74	6 0 0	1.971	1.971
47.054	12	0 3 0	1.930	1.925
47.773	70	−2 0 4	1.902	1.903
48.310	21	4 2 1	1.882	1.882
plus 22 lines to d(obs) = 1.238				

TABLE III

POSITIONAL[a] AND ANISOTROPIC THERMAL[b] PARAMETERS FOR THE ATOMS OF $Y_5Mo_2O_{12}$

Atom	Position	x	y	z	B_{11}	B_{22}	B_{33}	B_{12}	B_{13}	B_{23}
Mo(1)	4g	0(0)	0.7183(1)	0(0)	0.21(2)	0.43(1)	0.20(2)	0.00(0)	−0.02(1)	0.00(0)
Y(1)	4i	0.19364(6)	0.0(0)	0.36027(9)	0.25(5)	0.37(2)	0.20(2)	0.00(0)	−0.07(2)	0.00(0)
Y(2)	4i	0.81488(8)	0.0(0)	0.17640(9)	0.23(2)	0.42(2)	0.34(2)	0.00(0)	0.03(2)	0.00(0)
Y(3)	2d	0(0)	0.5000(0)	0.5000(0)	0.28(3)	0.64(4)	0.18(3)	0.00(0)	−0.02(3)	0.00(0)
O(1)	8j	0.6630(3)	0.2544(7)	0.0818(5)	0.21(11)	0.71(14)	0.49(12)	0.03(11)	0.06(10)	−0.02(11)
O(2)	8j	0.8454(3)	0.7513(7)	0.4245(5)	0.5(1)	0.4(1)	0.4(1)	0.1(1)	0.0(1)	0.1(1)
O(3)	4i	0.5002(4)	0(0)	0.7971(7)	0.7(2)	0.8(2)	0.3(2)	0.0(0)	0.2(1)	0.0(0)
O(4)	4i	0.0006(4)	0(0)	0.1816(7)	0.3(2)	0.6(2)	0.2(2)	0.0(0)	0.1(1)	0.0(0)

[a] Space group $C2/m$.
[b] $\exp[-0.25(B_{11}h^2a^{*2} \ldots + 2(B_{12}hka^*b^* \ldots))]$.

the 877 independent reflections, 138 violated the C-centering extinction condition. The average normalized structure factor, $\langle E^2 \rangle$, for reflections with $h + k = 2n + 1$ was 0.04 as calculated using NORMAL (*18*); this compares with a value of 1.97 for the $h + k = 2n$ reflections. As a consequence, the weak data were temporarily removed, and the structure determined by using the heavy-atom Patterson method in space group $C2/m$ (No. 12). Full-matrix least-squares refinement on all positional and anisotropic thermal parameters including terms for anomalous dispersion for all atoms and for anisotropic extinction converged with $R = 0.029$ and $R_w = 0.035$. Metal atom occupation factors were also refined and they confirmed the sites to be fully occupied. The largest peak in a final difference Fourier corresponded to 0.38 $e/Å^3$ and was located near an yttrium atom.

When all the data were included, the systematic absences were compatible with space group $P2_1/m$ (No. 11). Additional yttrium and oxygen atoms had to be placed in the asymmetric unit due to the lower symmetry. As expected, the positional and thermal parameters for these atoms were then strongly correlated. Several oxygen atoms displayed nonpositive definite isotropic thermal parameters while the correlated O atoms showed high isotropic B's. Also, the yttrium atoms could not be refined anisotropically. The oxygen isotropic temperature factors were then constrained at 0.5, and only molybdenum was refined anisotropically. Least-squares refinement converged at $R = 0.058$ and $R_w = 0.079$ with the largest residual in a difference map of 2.76e/Å^3 located near a yttrium atom. Overall standard deviations were 3–5 times higher than the C-centered refinement.

A study of both the $C2/m$ and $P2_1/m$ atomic positions and thermal parameters did not show any significant difference between the two structures. Any information that could have been derived from the additional weak reflections in $P2_1/m$ is probably masked by the correlation effects. Only the results of the $C2/m$ refinement are discussed below.

Results and Discussion

1. Structural Description

Atomic positional and thermal parameters are given in Table III, and important interatomic distances and angles are shown in Table IV.

$Y_5Mo_2O_{12}$ contains chains of distorted edge-shared MoO_6 octahedra extended along the monoclinic b axis. In this direction, the molybdenum atoms are spaced with alternating short and long distances of 2.496(1) and 3.221(1) Å. The short distance

TABLE IV

SELECTED INTERATOMIC DISTANCES (Å) AND ANGLES (deg) IN $Y_5Mo_2O_{12}$

Mo–Mo	2.496(1)	Y2–O1′	2.470(4)
Mo–Mo	3.221(1)	Y2–O1	2.293(4)
Mo–O1	1.908(3)	Y2–O2	2.275(4)
Mo–O3	1.966(4)	Y2–O4	2.261(5)
Mo–O4	2.106(3)		
		Y3–O2	2.303(4)
Y1–O1	2.444(4)	Y3–O3	2.223(5)
Y1–O2′	2.278(4)		
Y1–O2	2.307(4)		
Y1–O4	2.326(5)		
Mo–Mo–Mo	180.0	Y1–O2–Y3	123.0(1)
		Y1–O2–Y3	102.3(2)
Mo–O1–Y1	101.8(1)	Y2–O2–Y3	120.3(1)
Mo–O1–Y2	134.2(2)		
Mo–O1–Y2	99.6(1)	Mo–O3–Mo	78.8(2)
Y1–O1–Y2	108.4(1)	Mo–O3–Y3	140.6(1) (2×)
Y1–O1–Y2	101.9(1)		
Y2–O1–Y2	109.1(1)	Mo–O4–Mo	99.8(2)
		Mo–O4–Y1	99.9(2) (2×)
Y1–O2–Y1	101.8(1)	Mo–O4–Y2	100.7(2) (2×)
Y1–O2–Y2	99.6(1)	Y1–O4–Y2	147.8(2)
Y1–O2–Y2	107.8(1)		

represents a molybdenum–molybdenum bond. Almost identical octahedral chains are found in the distorted-rutile structure of MoO_2 which displays Mo–Mo separations

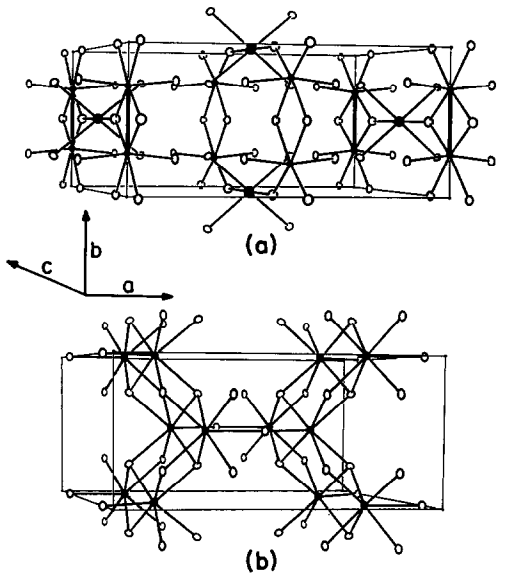

FIG. 1. The unit cell of $Y_5Mo_2O_{12}$ showing (a) only the rutile-like sheets of edge- and corner-shared octahedra of MoO_6 and YO_6; (b) only the interconnecting YO_7 monocapped trigonal prisms.

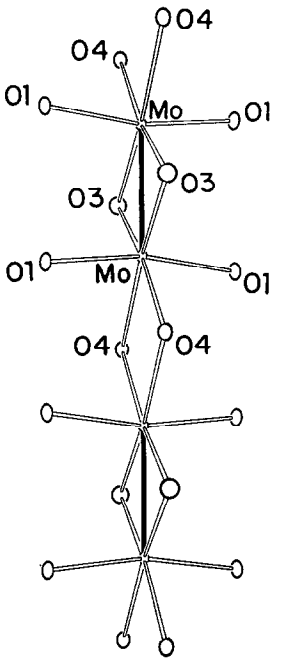

FIG. 2. A section of an edge-shared MoO_6 octahedral chain showing the Mo–Mo bonds in $Y_5Mo_2O_{12}$.

of 2.511 and 3.112 Å (*19*). In addition, the chains in MoO_2 are slightly puckered (Mo–Mo–Mo angle is 172.6°) while they are linear in $Y_5Mo_2O_{12}$. In the yttrium compound, YO_6 octahedra link the chains in the *bc* plane by sharing opposite oxygen corners (Fig. 1a). These planes are also related to those in the rutile structure but have yttrium atoms only in every other octahedral site along the *b* axis. The rutilelike planes are interconnected by sharing corners and edges with YO_7 monocapped trigonal prisms (Fig. 1b).

A section of an edge-shared octahedral MoO_6 chain showing the Mo–Mo bonds is given in Fig. 2. In $Y_5Mo_2O_{12}$, each molybdenum is in a formal oxidation state of +4.5, and has 1.5 electrons available for metal–metal bonding. Oxygen atom O3 bridges the short Mo–Mo separation and also forms a bond to yttrium. Due to its trigonal planar arrangement, this oxygen atom may be considered sp^2-hybridized.

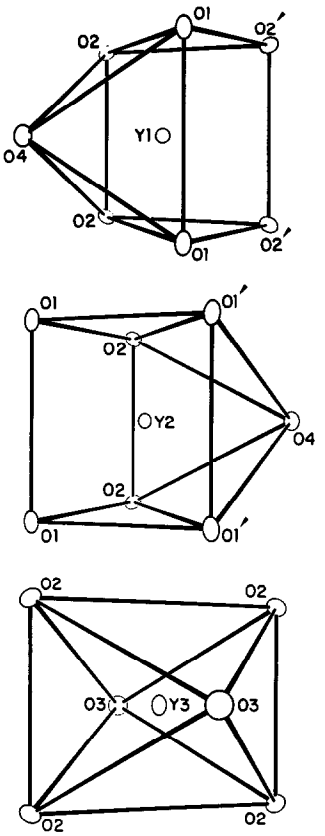

FIG. 3. Coordination polyhedra of the three crystallographic yttrium atoms in $Y_5Mo_2O_{12}$.

The sum of the Mo–O–Mo and Mo–O–Y bond angles around O3 is 360.0°. All other oxygen atoms in the structure are four-coordinated and may be considered sp^3-hybridized with average bond angles ranging 108.1–109.2° (Table IV). Atom O1 forms bonds with one Mo and three Y atoms, O2 is shared with four Y atoms, and O4 bonds to two Mo and two Y atoms. A major difference between the edge-shared octahedral chains in $Y_5Mo_2O_{12}$ and those in MoO_2 is the coordination symmetry of the O4 atoms that bridge the long Mo–Mo distance. In the yttrium compound, they are tetrahedrally coordinated. In MoO_2, all oxygen atoms are in a trigonal planarlike coordination (sp^2-hybridized) and have a lone p orbital available for π bonding with molybdenum.

The coordination of the three crystallographic yttrium atoms is shown in Fig. 3. Y1 and Y2 are each bonded to seven oxygen atoms in monocapped trigonal prismatic (C_s) symmetry with the capping atom on one of the rectangular faces. Y3 is bonded to six O atoms in approximately octahedral (C_{2h}) symmetry and is the link between the MoO_6 chains. The average Y–O bond distances of 2.34 Å for Y1, 2.33 Å for Y2, and 2.28 Å for Y3 compare well with the sum of ionic radii (*20*); 2.34 Å for 7-coordinate Y, and 2.27 Å for 6-coordinate Y. The structure of $Y_5Mo_2O_{12}$ is essentially indentical with that found for $Dy_5Re_2O_{12}$, particularly with regard to the transition metal chains (*16*). The coordination polyhedra of the rare-earth ion by oxygen are also similar although some marked differences in bond lengths are noted which may be due to the inability to completely refine the structure of the rhenium compound.

The valence of each independent atom in $Y_5Mo_2O_{12}$ was calculated by a summation of the bond strengths for that atom. This type of calculation has recently been used to estimate metal oxidation states (*21, 22*) and π bonding effects (*21*) in molybdenum atom cluster oxides. Bond strengths were calculated using

$$s = (d/d_0)^{-N}$$

where s = strength of a particular bond, d = crystallographic bond length, d_0 = length of a bond of unit valence, and N is a fitted constant. Values for d_0 and N were taken from Brown (*23*):

Mo–O bonds:	1.882 and 6.0
Y–O bonds:	2.070 and 7.0.

For Mo, Y1, Y2, and Y3, the calculated oxidation states are +4.40, +3.03, +3.13, and +3.11, respectively. The value for molybdenum is close to that based on the stoichiometry (+4.5). Calculated valences for

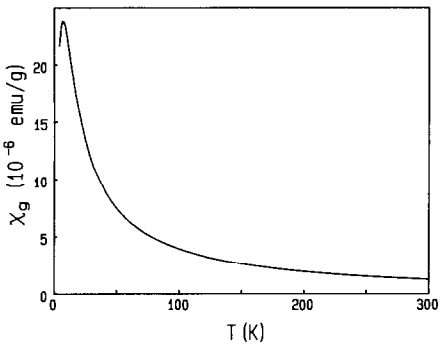

FIG. 4. Magnetic susceptibility of $Y_5Mo_2O_{12}$ as a function of absolute temperature.

O1, O2, O3, and O4 are 2.01, 1.97, 2.15, and 2.00, respectively. The value for trigonally planar O3 is higher than expected for sigma bonds only (i.e., a valence sum of 2.0) and suggests a π-bonding interaction with molybdenum. However, it is interesting to note that the Mo–O3 bond length of 1.966(4) Å is significantly longer than the Mo–O1 distance of 1.908(3) Å in which O1 is sp^3-hybridized. The shortening may be the result of a synergistic effect whereby the formation of the Mo–O3 π bond lowers O1–O3 repulsions and results in a strengthened Mo–O1 σ bond, albeit at the expense of the Mo–O4 σ bond.

2. Magnetic and Electrical Properties

A plot of the magnetic susceptibility of $Y_5Mo_2O_{12}$ vs temperature is shown in Fig. 4. The data can be fit to $\chi = C_g/(T + \theta) + \chi_0$ over the temperature interval from 15–300 K where $C_g = 437 \times 10^{-6}$ emu–K/g, $\theta = 7.5$ K, and $\chi_0 = -0.151 \times 10^{-6}$ emu/g for 202 experimental points with a mean square deviation of 0.26%. A value of $\mu_{eff} = 1.70\beta$ is found and corresponds very well to one unpaired electron per Mo_2 group. This is in accord with the observed average oxidation state of +4.5 for Mo in which a strong metal–metal bond is present. The peak in the susceptibility at 6 K indicates that the unpaired spins order antiferromagnetically, consistent with the positive Weiss constant obtained from the fit of the curve above 15 K.

The plot of electrical resistivity vs $1/T$ for both $Y_5Mo_2O_{12}$ and $Gd_5Mo_2O_{12}$ (Fig. 5) shows that both compounds are semiconductors with similar room temperature resistivities of 4.3×10^3 and 1.3×10^3 ohm–cm. Measurements are considered uncertain to about 30% due to uncertainties in defining crystal dimensions and current paths. The curves are approximately linear and their slopes correspond to carrier activation energies of 0.29 and 0.22 eV for the Y and Gd compounds, respectively. Low temperature measurements were terminated when nonohmic effects became apparent. Qualitative observations of the sign of the Seebeck coefficient in the room-temperature neighborhood indicate that the majority carriers are electrons.

It is clear from the magnetic susceptibility data that each Mo_2 unit in $Y_5Mo_2O_{12}$ possesses one localized unpaired electron. This is also consistent with the observed high resistivity. In comparison, MoO_2, which contains related molybdenum atom strings, is metallic (*24*). Each molybdenum atom in MoO_2 has one electron available for Mo–Mo σ bonding and an additional electron for Mo–Mo π bonding. An energy-level diagram for this compound has been discussed (*24*). Electrical conductivity in MoO_2 is attributed to an overlap of molybdenum-based orbitals with an empty Mo–O π^* band arising from the p orbitals of otherwise sp^2-hybridized oxygen atoms. In $Y_5Mo_2O_{12}$, Mo–O π bonding is localized to the Mo_2 units because these dimers are "insulated" along the octahedral chains by sp^3-type oxygen atoms, and between chains by Y^{3+} ions. The shorter Mo–O3 bridge bond of 1.966(4) Å compared to 1.990 Å (ave) in MoO_2 may reflect a stronger Mo–O π interaction as well as a higher charge on molybdenum (+4.5 vs +4.0).

The Mo–Mo bond distance in $Y_5Mo_2O_2$ is

0.015 Å shorter than that in molybdenum dioxide (*19*) even though the yttrium compound contains one less electron per Mo_2 unit for metal–metal bonding. This may be explained by stronger Mo–Mo π bonding. The loss of ability to form Mo–O π bonds between dimeric units in the new compound may result in more extensive d–d π orbital overlap within the dimers and explain why the Mo–Mo nonbonded distance in this compound is 0.11 Å longer than in MoO_2. As a result, this localized molecular orbital, which contains the unpaired electron, would lie at a relatively lower energy level, and the Mo–Mo bond lengths could remain approximately the same. In other words, the energy lost by removal of one π-bonding electron from its molecular orbital may be balanced by a lowering of that orbital's energy.

3. *Chemical Modifications*

In order to ascertain whether the molybdenum could be reduced further, the synthesis of $ZrY_4Mo_2O_{12}$ and $ZrGd_4Mo_2O_{12}$ was attempted using both solid-state reactions and fused salt electrolysis. The solid-state preparations in which stoichiometric quantities of reactants were fired in evacuated sealed silica capsules for 3- to 5-day periods each of 1000, 1100, and 1225°C periods, yielded copperish-looking materials which appeared visually homogeneous under 50× magnification. The color is in marked contrast to the green–blue color of powdered samples of both $Y_5Mo_2O_{12}$ and $Gd_5Mo_2O_{12}$. However, the X-ray powder diffraction patterns of the zirconium-containing materials show that, in addition to MoO_2, two other phases are present at approximately equal intensities of the principal peaks: (1) a rare-earth-stabilized cubic ZrO_2 phase with a slightly larger lattice constant than pure cubic ZrO_2; and (2) the $Ln_5Mo_2O_{12}$-type phase with somewhat broadened lines but with essentially the same although perhaps slightly smaller lattice parameters as the undoped phase (i.e., differences are within the ESD's of the results).

Fused salt electrolysis, in which 3 mole% ZrO_2 was substituted for the rare-earth oxide in the reaction mixture, yielded $Ln_5Mo_2O_{12}$-like crystals. The X-ray powder diffraction patterns of the purified cathode products from both the Y and Gd systems gave no evidence for any substantial substitution by Zr although the lines were again notably broadened. The crystals in both systems upon grinding yielded a light copper-colored powder. Further, the resistivity as a function of temperature for one of the crystals taken from the Gd:Zr system is virtually identical with that of a pure $Gd_5Mo_2O_{12}$ crystal (Fig. 5).

It would therefore appear that reduction of Mo to the tetravalent state is not favored. Although some zirconium substitution appears to take place based both upon the color change and the broadening of the diffraction lines, it is quite limited and has no effect on the conduction process.

Although mixed valence oxides in which the transition metal cations are located on crystallographically equivalent sites are unusual, they are nonetheless well established (*25, 26*). Perhaps the best understood example is $La_4Re_6O_{19}$ (*27, 28*) where the average oxidation state for rhenium is +4.33. Again, the dominant feature of this structure is pairs of ReO_6 octahedra which result in discrete Re–Re dimers with a bond distance of 2.42 Å, compatible with a double bond. These Re_2O_{10} groups, rather than forming chains, link to each other by sharing corners, resulting in a complex three-dimensional array in which the Re–O network provides a mechanism for electron delocalization (*29*). The nonbonding d electrons occupy this band and the compound is a metal. On the other hand, in $Y_5Mo_2O_{12}$ only localized Mo–Mo and Mo–O π-bonding is possible and the compound is a semiconductor.

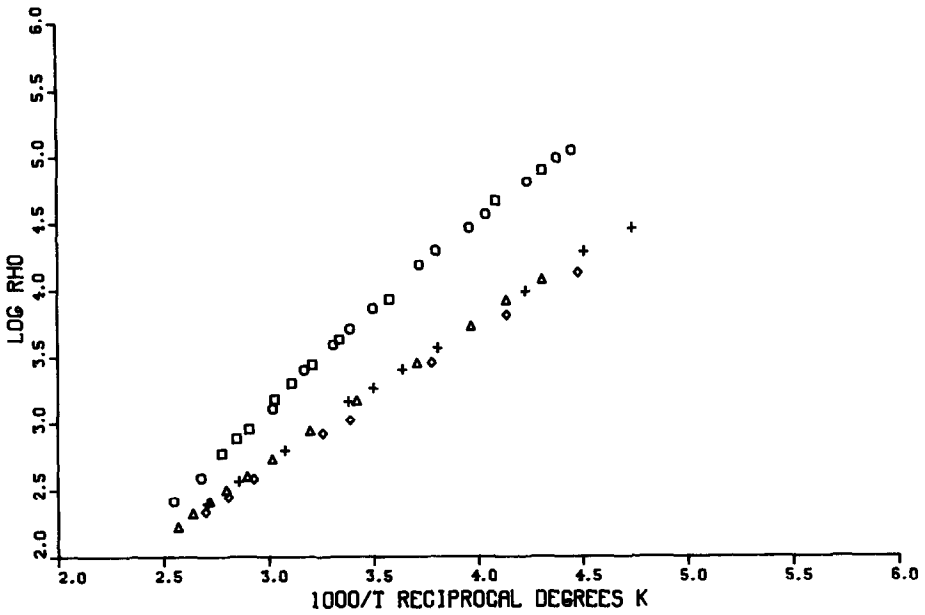

FIG. 5. Variation of log resistivity vs reciprocal of absolute temperature for $Ln_5Mo_2O_{12}$ phases: $Y_5Mo_2O_{12}$ heating—□, cooling—○; $Gd_5Mo_2O_{12}$ heating—△, cooling—+; Zr-doped $Gd_5Mo_2O_{12}$ cooling—◇.

Acknowledgments

The authors thank C. M. Foris for obtaining the Guinier film data. C.F. and W.H.M. are grateful for a grant from Research Corporation for supplies and equipment.

References

1. E. BANKS AND M. NEMIROFF, *Inorg. Chem.* **13,** 2715 (1974).
2. P-H. HUBERT, *Bull Soc. Chim Fr.*, 2385 (1974).
3. P-H. HUBERT, *Bull Soc. Chim Fr.*, 475 (1975).
4. H. KERNER-CZESKLEBA AND G. TOURNE, *Bull. Soc. Chim Fr.*, 729 (1976).
5. H. KERNER-CZESKLEBA AND G. TOURNE, *Mater. Res. Bull.* **13,** 271 (1978).
6. H. KERNER-CZESKLEBA AND B. CROS, *Mater. Res. Bull.* **13,** 947 (1978).
7. H. KERNER-CZESKLEBA, "Third Annual Conference on The Chemistry and Uses of Molybdenum," (Ann Arbor), p. 137 (1979).
8. A. MANTHIRAM AND J. GOPALAKRISHNAN, *Indian J. Chem. A,* **19,** 1042 (1980).
9. A. MANTHIRAM AND J. GOPALAKRISHNAN, *J. Less-Common Met.* **68,** 167 (1979).
10. H. CZESKLEBA-KERNER, B. CROS AND G. TOURNE, *J. Solid State Chem.* **37,** 294 (1981).
11. A. MANTHIRAM AND J. GOPALAKRISHNAN, *J. Less-Common Met.* **99,** 107 (1984).
12. M. A. SUBRAMANIAN, G. ARAVAMUDAN, AND G. V. SUBBA RAO, *Prog. Solid State Chem.* **15,** 55 (1983).
13. O. MULLER AND R. ROY, *Mater. Res. Bull.* **4,** 349 (1969).
14. W. H. MCCARROLL, C. DARLING, AND G. JAKUBICKI, *J. Solid State Chem.* **48,** 189 (1983).
15. G. BAUD, J-P. BESSE, R. CHEVALIER, AND M. GASPERIN, *Mater. Chem. Phys.* **8,** 93 (1983).
16. G. BAUD, J-P. BESSE, M. CAPESTAN, AND R. CHEVALIER, *Ann. Chim. Fr.* **7,** 615 (1982).
17. F. J. DISALVO, S. A. SAFRON, R. C. HADDON, J. V. WASZCZAK, AND J. E. FISCHER, *Phys. Rev. B* **20,** 4883 (1979).
18. P. MAIN, L. LESSINGER, M. M. WOOLFSON, G. GERMAIN, J. P. DECLERG, "MULTAN 78: A System of Computer Programs for the Automatic Solution of Crystal Structures from X-ray Diffraction Data," York, England and Louvain-la-Neuve, Belgium (1978).
19. B. G. BRANDT AND A. C. SKAPSKI, *Acta Chem. Scand.* **21,** 661 (1967).
20. R. D. SHANNON, *Acta Crystallogr. A* **32,** 751 (1976).

21. C. C. TORARDI AND J. C. CALABRESE, *Inorg. Chem.* **23,** 3281 (1984).
22. R. E. MCCARLEY, K.-H. LII, P. A. EDWARDS, AND L. F. BROUGH, *J. Solid State Chem.* **57,** 17 (1985).
23. I. D. BROWN, *"Structure and Bonding in Crystals,"* Vol. II (O'Keefe and Navrotsky, Eds.), Academic Press, New York (1981).
24. D. B. ROGERS, R. D. SHANNON, A. W. SLEIGHT, AND J. L. GILLSON, *Inorg. Chem.* **8,** 841 (1969).
25. F. ABRAHAM, J. TREHAUX, AND D. THOMAS, *J. Solid State Chem.* **29,** 73 (1979).
26. F. A. COTTON AND C. E. RICE, *J. Solid State Chem.* **25,** 143 (1978).
27. J. M. LONGO AND A. W. SLEIGHT, *Inorg. Chem.* **7,** 108 (1968).
28. N. L. MORROW AND L. KATZ, *Acta Crystallogr. B* **24,** 1466 (1968).
29. T. P. SLEIGHT, C. R. HARE, AND A. W. SLEIGHT, *Mater. Res. Bull.* **3,** 437 (1968).